

See discussions, stats, and author profiles for this publication at: <https://www.researchgate.net/publication/263954453>

Role of Metal Cations in Alkali Metal Chloride Doped Graphene

ARTICLE *in* THE JOURNAL OF PHYSICAL CHEMISTRY C · APRIL 2014

Impact Factor: 4.77 · DOI: 10.1021/jp500646e

CITATIONS

5

READS

48

4 AUTHORS, INCLUDING:



Ki Chang Kwon

Seoul National University

16 PUBLICATIONS 169 CITATIONS

[SEE PROFILE](#)



Kyoung Soon Choi

Chung-Ang University

21 PUBLICATIONS 201 CITATIONS

[SEE PROFILE](#)

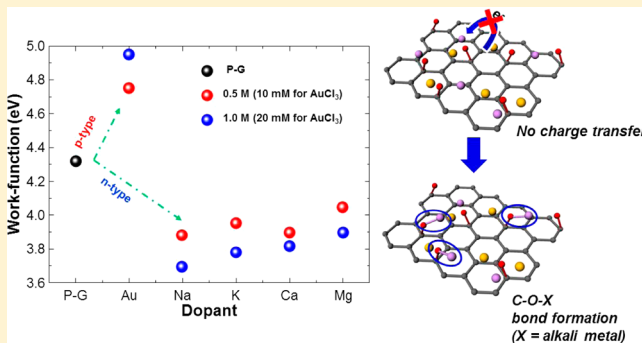
Role of Metal Cations in Alkali Metal Chloride Doped Graphene

Ki Chang Kwon, Kyoung Soon Choi, Cheolmin Kim, and Soo Young Kim*

School of Chemical Engineering and Materials Science, Chung-Ang University, 221 Heukseok-dong, Dongjak-gu, Seoul 156-756, Republic of Korea

Supporting Information

ABSTRACT: The doping mechanism of graphene with chlorides of low work-function metals was investigated using NaCl, KCl, MgCl₂, and CaCl₂. After graphene was doped with 1.0 M dopants, the sheet resistance of the graphene increased from 780 Ω sq⁻¹ to 1350–1620 Ω sq⁻¹ after doping. Its transmittance at 550 nm also decreased from 97% to 90–94% owing to the presence of metal particles. The shift of G and 2D peaks in the Raman spectra coincided with n-type doping phenomena. The shift of the peak for the C=C bond to high binding energy and the decrease of the $I_{C=C}/I_{C-C}$ intensity ratio in spectra acquired using synchrotron radiation photo-emission spectroscopy (SRPES) provided further evidence of n-type doping. Furthermore, secondary cutoff spectra in SRPES showed that the work function of the doped graphene progressively decreased from 4.32 eV to 3.7, 3.66, 3.81, and 3.9 eV. The formation of interfacial dipole complexes between the oxidized functional group on graphene and metal cations with low work functions is considered to induce n-type doping, resulting in a decrease of both the conductivity and work function of the graphene sheet. Therefore, metal cations may play an important role in an alkali or alkaline metal chloride doping system.



INTRODUCTION

Since graphene was discovered by a mechanical exfoliation method in 2004, there have been many reports describing graphene synthesis and its superior properties, such as the high mobility it affords to charge carriers, excellent thermal and electrical conductivity, and flexibility.^{1–3} To enable the use of graphene as a transparent conducting electrode, researchers have developed doping methods to reduce sheet resistance and increase the work function of graphene sheets. In general, graphene-doping methods can be categorized in three ways as follows. First, there is substitution doping, which mainly occurs during the graphene growth step.^{4–6} Boron and nitrogen atoms, which are located in the right and left side of carbon in the periodic table, are usually used as p- or n-type substitution dopants, respectively. The second method is charge-transfer doping between graphene and dopant molecules. In this method, organic materials with high electronegativity can induce surface charge transfer from graphene to their molecules because of an electronegativity difference.^{7–9} The third method is chemical doping that uses spontaneous charge transfer induced by the difference in electroreduction potential and negative Gibbs free energy.^{10–12}

Among these doping techniques, adsorption-induced chemical doping is an efficient Fermi-level engineering technique without basal plane reactions, thereby preventing any damage to the carbon networks. Metal chlorides, organic dopants, and metal oxide layers have been used as chemical dopants.^{13–15} In the case of metal chlorides, metal ions are spontaneously reduced to metal particles by accepting electrons from the

graphene sheet owing to their negative Gibbs free energy, thereby inducing the charge transfer.^{16,17} In our previous report, it was shown that the aggregation of metal particles and the adsorption of chlorine ions degraded the properties of graphene.¹⁸ Furthermore, the degree of doping was related to the electronegativity of the anion, and the degradation of the graphene was related to the bond strength between the cation and the counteranion.¹² However, these results were limited to the investigation of the role of cations and anions in metal chlorides where metals with high work functions were used. Therefore, it was concluded that an investigation of the role of cations and anions in chlorides with low work-function metals was necessary to thoroughly understand the general role of cations and anions. This type of experiment could elucidate the effect of bulk metal work function in metal chlorides on the degree of modified work function in metal chloride doped graphene.

In this article, we used a chemical vapor deposition (CVD) method to synthesize a graphene sheet. Alkali or alkaline earth metals (X-metal) with low work functions, such as Na (2.36 eV), K (2.29 eV), Ca (2.87 eV), and Mg (3.66 eV) were adopted as cations for the metal chlorides.¹⁶ Gold chloride containing a high work-function metal, Au (5.1 eV), was used as the control dopant material in this experiment. NaCl, KCl, MgCl₂, and CaCl₂ were dissolved in separate solutions with

Received: January 20, 2014

Revised: March 21, 2014

Published: March 26, 2014

deionized (DI) water at concentrations of 1 M. To investigate the effect of metal cations on graphene doping, the core level C 1s spectra were obtained using synchrotron radiation photoemission spectroscopy (SRPES); in addition, ultraviolet photoemission spectroscopy (UPS), four-point probe technique, and UV-visible spectroscopy were performed. Field-emission scanning electron microscopy (FE-SEM) and energy dispersive spectroscopy (EDS) were performed to investigate the surface of the doped graphene sheet. On the basis of these experimental results and measurements, the effects of the various cations of the metal chlorides on graphene doping and some suggested graphene doping mechanisms are discussed.

■ EXPERIMENTAL DETAILS

Graphene Film Preparation. Graphene samples were grown on a 25 μm thick copper foil in a quartz tube furnace, using a CVD method involving methane (CH_4) and hydrogen (H_2) gases. Under vacuum conditions of 90 mTorr, the furnace was heated without a gas flow for 30 min. Before the growth of graphene, copper foil was preheated at 950 °C for 30 min. To obtain a large single-crystal copper surface, H_2 gas was supplied to the furnace under a vacuum of 150 mTorr at a rate of 33 cm³/min (sccm). After the preheating step, a gas mixture of CH_4 and H_2 was supplied at a ratio of 200:33 sccm under ambient conditions for 10 min to synthesize the graphene. After 10 min of growth, the furnace was cooled to room temperature at a rate of 10–15 °C/min, under 33 sccm of H_2 flow. Poly(methyl methacrylate) (PMMA) was then spin-coated onto the graphene, and the PMMA-coated foil was heated on a hot plate heated to 180 °C for 1 min, after which O_2 plasma was used to etch the graphene on the other side of the copper foil. The sample was then immersed in a ferric chloride (1 M FeCl_3) bath at room temperature for 12–18 h to etch away the copper foil. Then, the remaining sample was carefully dipped into a DI water bath about 7–9 times to remove any residual etchant. The graphene sheets were then transferred onto an arbitrary substrate. PMMA was removed by immersion in an acetone bath at 50 °C for 30 min after the graphene layer had completely adhered to the target substrate.

Doping of Graphene Using Metal Chloride Solutions.

After the graphene sheet was transferred to a glass or Si/SiO₂ wafer substrate, the sample was set on the spin-coater. The X-metal chlorides (NaCl, KCl, CaCl₂, and MgCl₂) were separately dissolved in two solutions, each containing DI water, at concentrations of 0.5 and 1 M. The gold chloride (AuCl_3), which was used as reference dopant, was dissolved in two solutions of nitromethane at concentrations of 10 and 20 mM. A 1 mL amount of each of the X-metal chloride solutions with different concentrations were spin-coated on transferred graphene substrates at 1500 rpm for 1 min after a residual time of 1 min. In the case of AuCl_3 , 200 μL of AuCl_3 was spin-coated on the transferred graphene substrate at 2500 rpm for 1 min. Then, the samples were annealed at 150 °C on a hot plate for 30 min to evaporate the solvent.

Characterization. The sheet resistance was measured in a standard state using a four-point probe technique (Keithley 2612A multimeter, USA). UV-visible spectra were recorded on a JASCO V-740 photospectrometer with a wavelength range 400–900 nm. FE-SEM (JEOL, JSM-5410LV, Japan) images of the pristine and doped graphene films were also obtained. Raman spectra of graphene were obtained with a Lab RAM HR (Horiba JobinYvon, Japan) at an excitation wavelength of 514.54 nm. SRPES experiments were performed in an ultrahigh

vacuum chamber (base pressure of $\sim 10^{-10}$ Torr) in a 4D beamline, equipped with an electron analyzer and a heating element, at the Pohang Acceleration Laboratory. The onset of photoemission, corresponding to the vacuum level at the surface of graphene, was measured using an incident photon energy of 250 eV with a negative bias on the sample. The results were corrected for charging effects by using Au 4f as an internal reference.

■ RESULTS AND DISCUSSION

Figure 1a shows the change of sheet resistance (R_{sh}) of graphene sheet doped with metal chlorides containing different

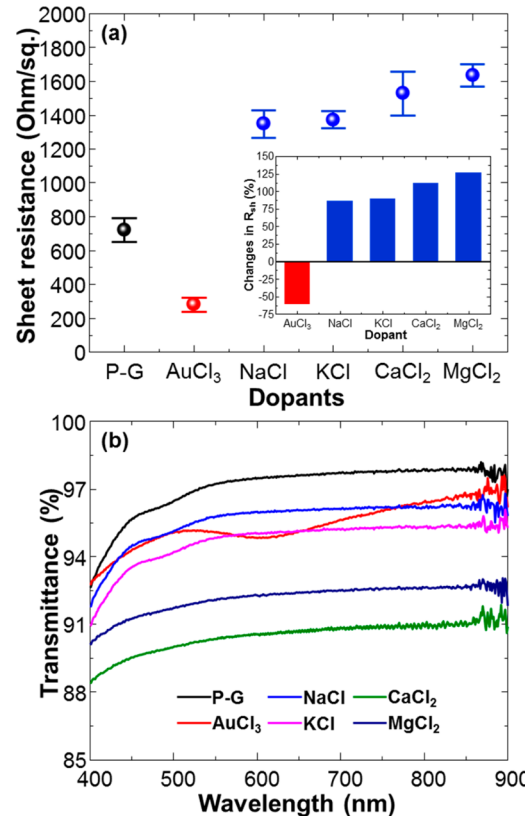


Figure 1. (a) Change of R_{sh} after doping of graphene sheets. The value of R_{sh} changes with the type of metal chloride as depicted in the inset figure. The largest and smallest increases of R_{sh} are about 125% for MgCl_2 and about 87.5% for NaCl, respectively. For AuCl_3 -doped graphene, R_{sh} decreases from 870 to 300 $\Omega \cdot \text{sq}^{-1}$. (b) Transmittance spectra of P-G and graphene doped with five types of X-metal and gold chlorides at a concentration of 1.0 M (20 mM for AuCl_3). The transmittance of P-G at 550 nm is 97.3%. The graphene doped with CaCl_2 at 550 nm shows the lowest transmittance of 90.3%.

types of cations. The R_{sh} of pristine graphene (P-G) was about 650–795 $\Omega \cdot \text{sq}^{-1}$ as displayed by the error bar. In the case of the graphenes doped with low work-function metal chlorides, R_{sh} increased to 1350, 1370, 1530, and 1630 $\Omega \cdot \text{sq}^{-1}$ for the NaCl-, KCl-, CaCl_2 -, and MgCl_2 -doped graphenes, respectively. The MgCl_2 -doped graphene showed the highest R_{sh} value, and all samples showed increased R_{sh} values compared with that of the P-G sample. However, R_{sh} was reduced to 330 $\Omega \cdot \text{sq}^{-1}$ for the graphene doped with AuCl_3 . The inset diagram of Figure 1a displays the changes in R_{sh} with respect to the type of the dopant used. All the R_{sh} values of the low work-function metal chloride doped samples increased up to 120% of that of the P-

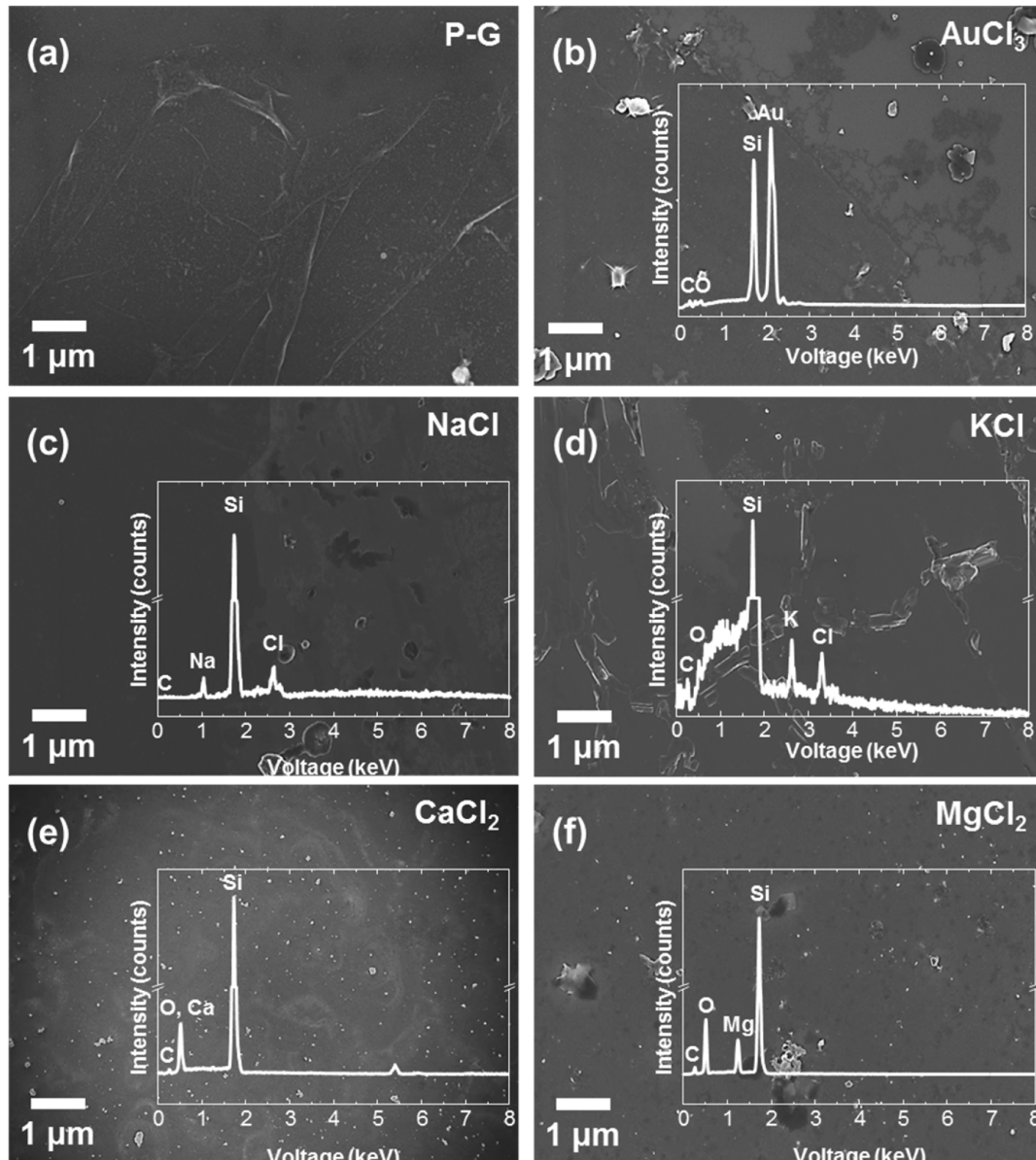


Figure 2. SEM images and EDS spectra of graphenes doped with 1.0 M (20 mM for AuCl_3) solutions. There are some wrinkles and ripples in the FE-SEM images of P-G. The metal particles, which are not observed in P-G, originate from the doping solution. The SEM image and EDS spectrum of each different metal chloride doped graphene are displayed: (a) pristine, (b) AuCl_3 , (c) NaCl , (d) KCl , (e) CaCl_2 , and (f) MgCl_2 -doped graphene sheets.

G sample. This result suggested that the metal chlorides with high work-function metals decreased the R_{sh} of graphene, while the metal chlorides with low work-function metals increased the R_{sh} of graphene. It is reported that P-G has p-type properties.¹⁹ Therefore, it is thought that metal chlorides with high work-function metals make graphene have p-type properties, while the metal chlorides with low work-function metals make graphene have n-type properties. Figure 1b shows the transmittance of the graphene sheets doped with each metal chloride. The transmittance at 550 nm of P-G was about 97%. It is shown that the transmittance at 550 nm of doped samples decreased to 95.6% for NaCl and 90.2% for CaCl_2 . The transmittance at 550 nm of the AuCl_3 -doped graphene also decreased to 95.3%. The decrease of transmittance is induced by metal particles on doped graphene sheets after the solvent evaporation process. Therefore, it is concluded that the metal

chlorides reduced the transmittance of the graphene regardless of the type of metal present in the metal chloride.

To investigate the surface changes in the doped graphenes, FE-SEM and EDS measurements were performed, as shown in Figure 2. The wrinkles and ripples seen on the P-G sheet are typical of a graphene sheet. However, particles that are absent on the P-G sheet are observed on the surface of the doped graphene sheets. The EDS spectra indicate that these metal particles originated from the doping solution. The metal particles on the doped graphene sheets are uniformly dispersed, indicating that the positive charges of the metal ions in the metal chlorides cause the formation of metal particles on the graphene surface. In EDS spectra, it should be noted that a strong oxygen peak was detected in graphene doped with KCl , CaCl_2 , and MgCl_2 except AuCl_3 . Therefore, it is thought that

the graphene was well doped after each different metal chloride treatment.

Figure 3 shows the Raman spectra of doped graphene and comparison graphs for its G and 2D peaks. The dashed line in

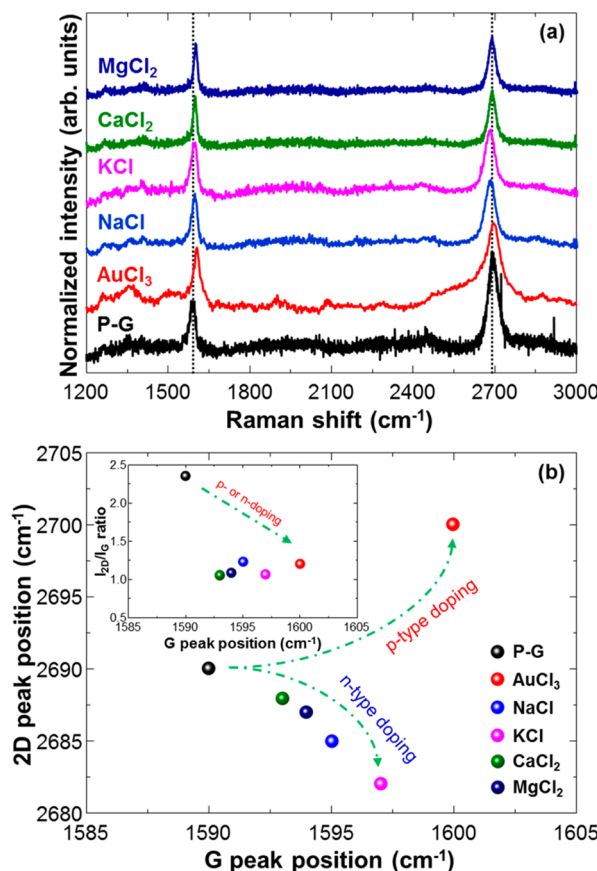


Figure 3. (a) Raman spectra of each metal chloride doped graphene sheet. In the case of the G peak, the peak shifts to higher wavenumbers in all samples, indicating the efficient graphene doping with the dopant solution. In the case of the 2D peak, the peak shifts to lower wavenumbers. The 2D peak of the AuCl₃-doped graphene shifts to a higher wavenumber. (b) Scatter plots for the positions of the G and 2D peaks in Raman spectra with data points adapted from P-G and doped graphene samples. A green curved line is added for facilitating visual comparison.

Figure 3a indicates the position of the G and 2D peaks in the P-G sheet. First, there is no D peak in any of the doped graphene sheets, indicating that the basal plane reactions or substitution impurities were not caused by metal chloride dopants. Second, the G peak position of P-G is revealed at 1590 cm⁻¹. In the case of all the doped graphenes including AuCl₃, the G peaks are significantly shifted to higher wavenumbers of about 10, 5, 7.5, 2.5, and 3.5 cm⁻¹ for AuCl₃, NaCl, KCl, CaCl₂, and MgCl₂, respectively. The 2D peak positions of the graphenes doped with NaCl, KCl, CaCl₂, and MgCl₂ are shifted to lower wavenumbers, compared to the higher wavenumber shift of the AuCl₃-doped graphene. The G and 2D peaks are plotted together to clarify the changes in peak positions and to compare the peaks of the AuCl₃-doped graphene with those of the others, as shown in Figure 3b. Both electron- and hole-doping on graphene have been reported to shift the G peak to higher wavenumbers.^{17,20} The calculation based on density functional theory revealed that the position of the 2D peak is

predicted to decrease for an increasing electron concentration.¹⁷ It means that the 2D peak shifts to high wavenumber for p-type doping but to low wavenumber for n-type doping. This allows the use of the 2D peak to discriminate between n-type and p-type doping. The green dashed curves are inserted to show the types of graphene doping using each different dopant material, according to the previously reported Raman analyses of doped graphenes.²⁰ The shifts of the G and 2D peaks in the Raman spectra of the NaCl-, KCl-, CaCl₂-, and MgCl₂-doped graphenes indicated that metal chlorides with low work-function metals contributed to the formation of a graphene n-type material. Additionally, the ratio of the intensities of the 2D peak to those of the G peaks significantly decreased after p- or n-type doping as shown in the inset graph of Figure 3b, which is consistent with previous reports.¹⁷ The large peak shifts and the significant intensity ratio changes in the 2D and G peaks of the doped graphene indicated that the graphenes were doped as n-type materials using each different doping material except AuCl₃.

To compare the changes in the core levels of the C 1s peaks in the SRPES spectra, the C 1s peak of each metal chloride doped graphene is shown in Figure 4a. The C 1s peak of P-G was separated into four components: sp² carbon (C=C) at 284.5 eV, sp³ carbon (C—C) at 285.5 eV, (C—O) at 286.7 eV, and a carbonyl group (C=O) near 289.0 eV.²¹ Although the P-G samples were synthesized using a CVD process, an oxidized carbon peak was found in the C 1s spectra because of the transfer process that used acetone, isopropyl alcohol, and DI water. The peak shift took place in each different metal chloride doped graphene, but this shift did not occur for P-G. The shift of the C=C peak position in each sample is summarized in Figure 4b for different dopant types. In the case of the AuCl₃-doped graphene, the C=C peak shifted from 285.4 to 284.2 eV, which is similar to the p-type doped case of carbon nanotubes.²² The shift of C 1s spectra to lower binding energy means the increase of work function, suggesting that the carbon atoms of the graphene donated their free electrons to Au³⁺ ions and consequently the graphene changed to a p-type material because of negative Gibbs free energy.²³ In contrast, the other X-metal cations could not spontaneously capture electrons from carbon atoms in the graphene networks because of their stable electron state of carbon that follows the octet rule, resulting in no reaction between ionic chlorine and uncharged carbon atoms. Therefore, the C=C peaks of the other X-metals shifted to a higher binding energy region, that is, from 285.4 eV to 285.3, 285.2, 285.3, and 285.0 eV for NaCl, KCl, CaCl₂, and MgCl₂, respectively. The variance in the ratio of C=C intensity to C—C intensity ($I_{C=C}/I_{C-C}$), as shown in Figure 4c, is one of the indicators that shows whether a graphene sample is doped. It has been reported that alkali carbonates have a significant tendency to combine the oxide functional group of carbon atoms with alkali metal ions.^{24–26} In these previous studies, it was found the interfacial dipole moment (C—O—X, X = alkali or alkaline earth metal) could act as an n-type dopant on the surface of graphene. The intensity of C—C significantly increased after X-metal chloride doping in our case, suggesting the combination of the carbons of the graphene with X-metal cations. However, in the case of AuCl₃, the $I_{C=C}/I_{C-C}$ intensity ratio increased after the doping treatment, proving that the electron transfer from the carbon atoms of the graphene to Au³⁺ ions occurred because of the positive reduction potential of the metal ions. These results indicate that the chlorides of X-metals imparted n-type

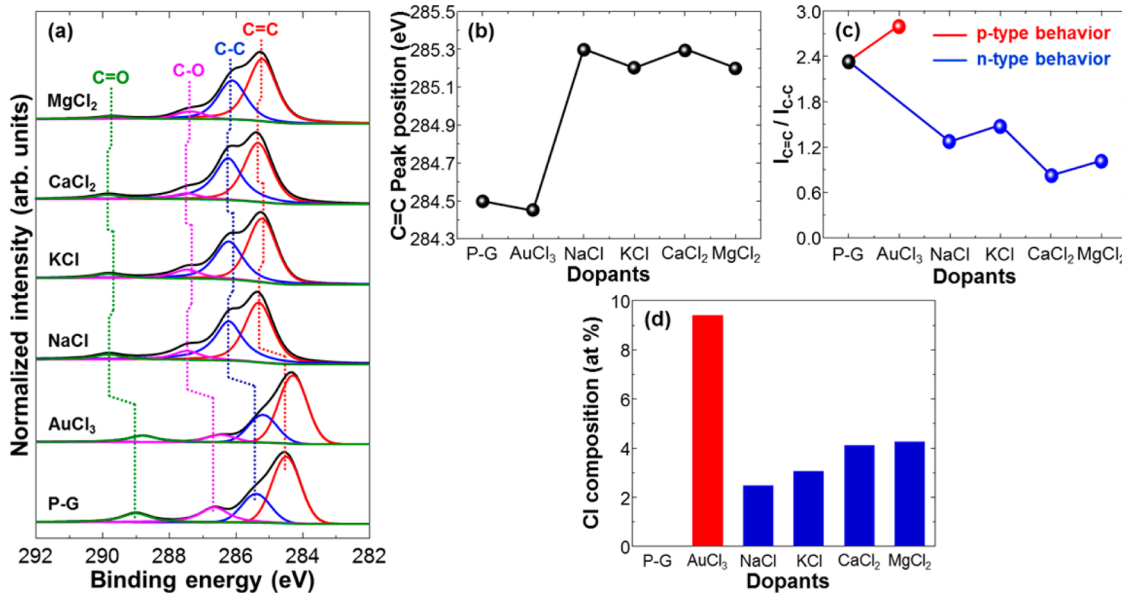


Figure 4. (a) SRPES C 1s spectra of each metal chloride doped graphene film. In the case of X-metal chloride doped graphene, the shifts of this peak to higher binding energies indicate the n-type doped state. (b) Shift of the peak corresponding to the C=C bond after each metal chloride doping process. (c) Ratio of $I_{C=C}/I_{C-C}$. The $I_{C=C}/I_{C-C}$ intensity ratio decreases after the doping treatment with X-metal chlorides, but that of the AuCl₃-doped graphene increases. (d) Atomic composition of Cl atoms in each metal chloride doped graphene sheet. The Cl composition of the X-metal chloride doped samples significantly decreases because of the absence of charge transfer between the metal cations and the carbon atoms.

properties to graphene. The atomic ratios of the chlorine atom in each doped graphene are displayed in Figure 4d. Each separated peak is shown in Figure SI1 (Supporting Information). The concentration of the Cl atoms in the AuCl₃-doped graphene was about 9%. However, the corresponding Cl ratios for the X-metal chloride doped graphenes were calculated to be less than 5%, suggesting that the Cl anions of these graphenes did not significantly react with carbon atoms. The electronegativity of Cl is higher than carbon in graphene. Therefore, it is thought that the amount of electron transfer from graphene to Cl anions in the X-metal chloride doped graphenes is less than AuCl₃-doped graphene.

Figure 5 shows the variance in the work functions of the graphenes doped with various dopants at concentrations of 0.5 and 1 M (10 and 20 mM for AuCl₃). The original data for the SRPES spectra, which were acquired in the regions of the secondary electron threshold, of graphenes doped with X-metal chlorides are shown in Figures SI2 and SI3 (Supporting Information). The corresponding secondary electron cutoff for AuCl₃ is also shown. The onset of the secondary electron cutoff energy was determined by extrapolating two straight lines from the background and threshold in the spectra.²⁷ The values of work function decreased from 4.32 eV to 3.7, 3.66, 3.81, and 3.9 eV upon doping with 1.0 M NaCl, KCl, MgCl₂, and CaCl₂, respectively. When more concentrated dopant solutions were used, lower work-function values were obtained. However, the work function of graphene doped with 20 mM AuCl₃ increased to 4.95 eV. These results indicate that chlorides with low and high work-function metals decreased and increased the work function of graphene, respectively. Therefore, the changes in the work functions for the metal chloride doped graphene sheets seem to be related to the work functions of the corresponding intrinsic bulk metals. The decrease of work function might be induced by the interfacial dipole moment of the C–O–X bond.

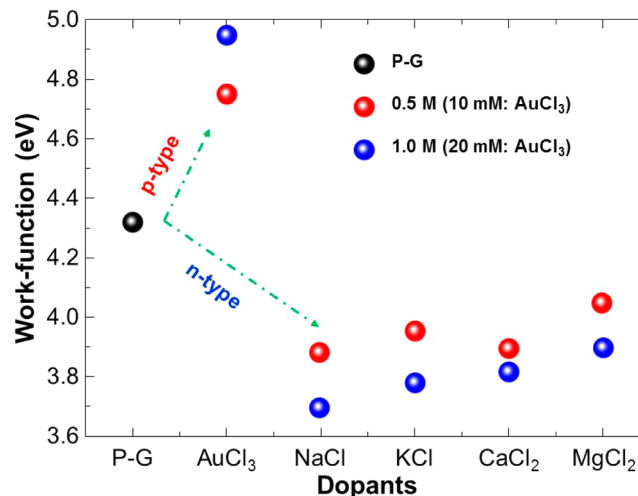


Figure 5. Work functions of graphenes doped with 0.5 and 1 M solutions (10 and 20 mM for AuCl₃) for different dopant metals. In X-metal chlorides, the work-function values decrease after doping, but that of the AuCl₃-doped graphene increases from 4.3 to 4.95 eV.

On the basis of these experimental observations, the n-type doping mechanisms of X-metal chloride doped graphene can be explained as follows. In the case of chlorides with high work-function metals such as gold, iridium, and rhodium chlorides (AuCl₃, IrCl₃, and RhCl₃), the metal cations in the dopant solutions spontaneously capture the electrons from the carbon atoms in the graphene sheet because of their negative Gibbs free energies, inducing the depletion of electrons in the graphene networks.¹⁰ Subsequently, the positively charged carbon atoms can easily react with chlorine anions in the dopant solutions, increasing the work function in each case. Additional depletion of electron in carbon atoms occurred due to the higher electronegativity of chlorine comparing with carbon atoms.²⁸ However, for the X-metal chlorides, the metal

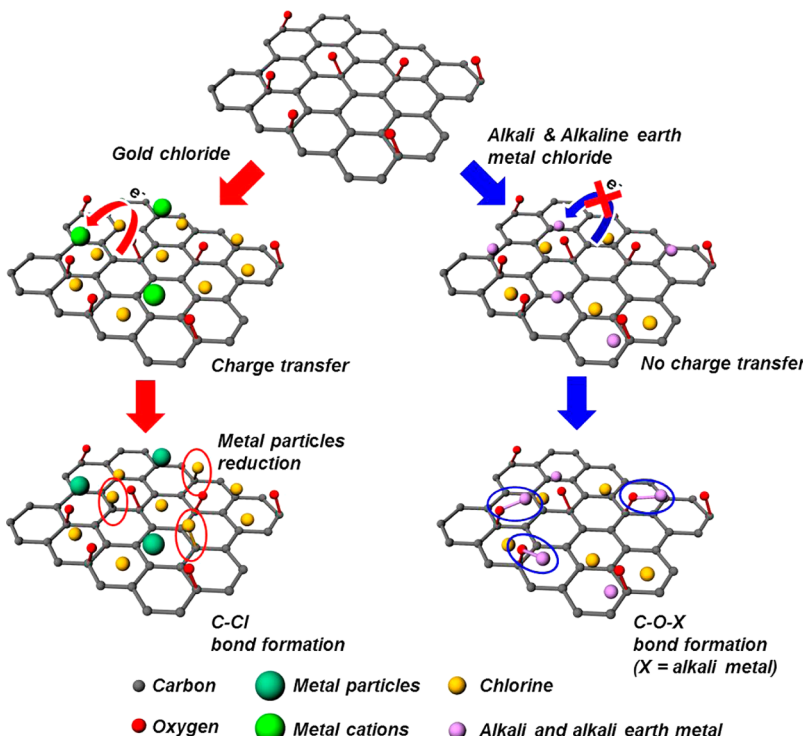


Figure 6. Suggested doping mechanism of graphene with X-metal chlorides compared with that of graphene with Au chloride.

cations in the dopant solutions cannot remove electrons from the graphene carbon atoms because of their stability according to the octet rule. Therefore, chlorine anions are difficult to be retained on the surface of graphene as shown in Figure 4d. From the SRPES analysis, it is evident that the intensity of the sp^3 carbon ($\text{C}-\text{C}$) peak significantly increased after doping with metal chlorides, suggesting the formation of $\text{C}-\text{O}-\text{X}$ bonds on the surface of the doped graphene. Furthermore, the peak position of the sp^2 carbon ($\text{C}=\text{C}$) was shifted to higher binding energy, and the secondary electron cutoffs in the UPS spectra were shifted to lower binding energies. The suggested doping mechanism is displayed in Figure 6. The $\text{C}-\text{O}-\text{X}$ bond forms interfacial dipole complexes on graphene surface. According to the electron tail reduction model, the work function could be altered with a surface dipole, which originates from the tail of free electrons. The contribution of this surface dipole could be modified by the presence of an adsorbate.²⁹ Therefore, interfacial complexes of $\text{C}-\text{O}-\text{X}$ bonds may act as additional adsorbates to reduce the value of the work function, converting the graphene into an n-type material.

CONCLUSION

The role of metal cations and the mechanism of X-metal chloride doping were investigated using different metal chloride solutions. The average sheet resistance value of X-metal chloride doped graphene increased from 650–795 to 1350–1630 $\Omega \text{ sq}^{-1}$. In general, the transmittance of the doped graphene sheets decreased due to metal particles. The G peak shifted to a higher wavenumber, and the 2D peak shifted to a lower wavenumber in the Raman spectra, regardless of the presence of X-metal chloride dopants, suggesting the n-type doping of graphene. Meanwhile, the peak shift of the $\text{C}=\text{C}$ bond to a higher binding energy and the decrease of the $I_{\text{C}=\text{C}}/I_{\text{C}-\text{C}}$ intensity ratio in the SRPES spectra provided further evidence of n-type doping. Furthermore, the secondary cutoffs

in the UPS spectra were shifted to lower binding energies, indicating a reduction in work functions. The formation of interfacial dipole complexes between the oxidized functional groups on graphene and X-metal cations might lead to n-type doping, resulting in a decrease of both the conductivity and work function of the graphene sheet. Therefore, metal cations may play an important role in alkali or alkaline metal chloride doping systems.

ASSOCIATED CONTENT

S Supporting Information

SRPES spectra of the Cl atoms; UPS spectra at concentrations of 0.5 and 1 M for alkali or alkaline earth metals and at concentrations of 10 and 20 mM for the AuCl_3 -doped graphene sheets. This material is available free of charge via the Internet at <http://pubs.acs.org>.

AUTHOR INFORMATION

Corresponding Author

*Phone: 82-2-820-5875; fax: 82-2-824-3495; e-mail: sooyoungkim@cau.ac.kr.

Notes

The authors declare no competing financial interest.

ACKNOWLEDGMENTS

This research was supported in part by the Basic Science Research Program (2011-0008994) and Mid-Career Research Program (2011-0028752) through the National Research Foundation of Korea (NRF) funded by the Ministry of Education, Science, and Technology, and in part by the Center for Green Airport Pavement Technology (CGAPT) of Chung-Ang University.

■ REFERENCES

- (1) Geim, A. K. *Science* **2009**, *324*, 1530–1534.
- (2) Geim, A. K.; Novoselov, K. S. *Nat. Mater.* **2007**, *6*, 183–191.
- (3) Du, X.; Skachko, I.; Barker, A.; Anderi, E. Y. *Nat. Nanotechnol.* **2008**, *3*, 491–495.
- (4) Hwang, J. O.; Park, J. S.; Choi, D. S.; Kim, J. Y.; Lee, S. H.; Lee, K. E.; Kim, Y.-H.; Song, M. H.; Yoo, S.; Kim, S. O. *ACS Nano* **2012**, *6*, 159–167.
- (5) Wang, X.; Li, X.; Zhang, L.; Yoon, Y.; Weber, P. K.; Wang, H.; Guo, J.; Dai, H. *Science* **2009**, *324*, 768–771.
- (6) Panchakarla, L. S.; Subrahmanyam, K. S.; Saha, S. K.; Govindaraj, A.; Krishnamurthy, H. R.; Waghmare, U. V.; Rao, C. N. R. *Adv. Mater.* **2009**, *21*, 4726–4730.
- (7) Lee, W. H.; Suk, J. W.; Chou, H.; Lee, J.; Hao, Y.; Wu, Y.; Piner, R.; Akinwande, D.; Kim, K. S.; Ruoff, R. S. *Nano Lett.* **2012**, *12*, 2374–2378.
- (8) Park, J.; Lee, W. H.; Huh, S.; Sim, S. H.; Kim, S. B.; Cho, K.; Hong, B. H.; Kim, K. S. *J. Phys. Chem. Lett.* **2011**, *2*, 841–845.
- (9) Jung, N.; Kim, N.; Jockusch, S.; Turro, N. J.; Kim, P.; Brus, L. *Nano Lett.* **2009**, *9*, 4133–4137.
- (10) Kwon, K. C.; Choi, K. S.; Kim, S. Y. *Adv. Funct. Mater.* **2012**, *22*, 4724–4731.
- (11) Shin, H.-J.; Choi, W. M.; Choi, D.; Han, G. H.; Yoon, S.-M.; Park, H.-K.; Kim, S.-W.; Jin, Y. W.; Lee, S. Y.; Kim, J. M.; Choi, J.-Y.; Lee, Y. H. *J. Am. Chem. Soc.* **2010**, *132*, 15603–15609.
- (12) Kwon, K. C.; Kim, B. J.; Lee, J.-L.; Kim, S. Y. *J. Mater. Chem. C* **2013**, *1*, 2463–2469.
- (13) Wang, Y.; Tong, S. W.; Xu, X. F.; Özyilmaz, B.; Loh, K. P. *Adv. Mater.* **2011**, *23*, 1514–1518.
- (14) Kwon, K. C.; Dong, W. J.; Jung, G. H.; Ham, J.; Lee, J.-L.; Kim, S. Y. *Sol. Energy Mater. Sol. Cells* **2013**, *109*, 148–154.
- (15) Wang, X.; Xu, J.-B.; Xie, W.; Du, J. *J. Phys. Chem. C* **2011**, *115*, 7596–7602.
- (16) Lide, D. R. *CRC Handbook on Chemistry and Physics*; CRC Press: Cleveland, OH, 2008; pp 12–114.
- (17) Das, A.; Pisana, S.; Chakraborty, B.; Piscanec, S.; Saha, S. K.; Waghmare, U. V.; Novoselov, K. S.; Krishnamurthy, H. R.; Geim, A. K.; Ferrari, A. C.; Sood, A. K. *Nat. Nanotechnol.* **2008**, *3*, 210–215.
- (18) Kwon, K. C.; Kim, B. J.; Lee, J.-L.; Kim, S. Y. *J. Mater. Chem. C* **2013**, *1*, 253–259.
- (19) Park, J.; Lee, W. H.; Huh, S.; Sim, S. H.; Kim, S. B.; Cho, K.; Hong, B. H.; Kim, K. S. *J. Phys. Chem. Lett.* **2011**, *2*, 841–845.
- (20) Wang, Q. H.; Jin, Z.; Kim, K. K.; Hilmer, A. J.; Paulus, G. L. C.; Shih, C.-J.; Ham, M.-H.; Sanchez-Yamaguchi, J. D.; Watanabe, K.; Taniguchi, T.; Kong, J.; Jarillo-Herrero, P.; Strano, M. S. *Nat. Chem.* **2012**, *4*, 723–732.
- (21) Benayad, A.; Shin, H.-J.; Park, H. K.; Yoon, S.-M.; Kim, K. K.; Jin, M. H.; Jeong, H.-K.; Lee, J. C.; Choi, J.-Y.; Lee, Y. H. *Chem. Phys. Lett.* **2009**, *475*, 91–95.
- (22) Despoja, V.; Sunjic, M. *Phys. Rev. B* **2013**, *88*, 245416–1–245416–9.
- (23) Dean, J. A. *Lange's Handbook of Chemistry*; McGraw-Hill Book Company: New York, 1979; pp 9:4–9:94.
- (24) Kwon, K. C.; Choi, K. S.; Kim, B. J.; Lee, J.-L.; Kim, S. Y. *J. Phys. Chem. C* **2012**, *116*, 26586–26591.
- (25) Huang, J.-H.; Fang, J.-H.; Liu, C.-C.; Chu, C.-W. *ACS Nano* **2011**, *5*, 6262–6271.
- (26) Pickett, W. E. *Phys. Rev. Lett.* **1994**, *73*, 1664–1667.
- (27) Kim, S. Y.; Hong, K.; Lee, J.-L. *Jpn. J. Appl. Phys.* **2005**, *50*, 101602-1–101602-4.
- (28) Kim, S. M.; Kim, K. K.; Jo, Y. W.; Park, M. H.; Chae, S. J.; Duong, D. L.; Yang, C. W.; Kong, J.; Lee, Y. H. *ACS Nano* **2011**, *5*, 1236–1242.
- (29) Kim, S. Y.; Hong, K.; Lee, J.-L. *Appl. Phys. Lett.* **2007**, *90*, 183508-1–183508-3.